Interaction of hagfish cathelicidin antimicrobial peptides with model lipid membranes

Gorka Basañez[a,b,*], Ann E. Shinnar[c], Joshua Zimmerberg[b]

[a] *Unidad de Biofísica (Centro Mixto UPV/CSIC), y Departamento de Bioquímica y Biología Molecular, Universidad del País Vasco (UPV/EHU), P.O. Box 644, 48080 Bilbao, Spain*

[b] *Laboratory of Cellular and Molecular Biophysics, National Institutes of Child Health and Human Development, NIH, Bethesda, MD 20892, USA*

[c] *Chemistry Department, Barnard College, New York, NY 10027, USA*

Received 3 September 2002; revised 22 October 2002; accepted 27 October 2002

First published online 7 November 2002

Edited by Maurice Montal

Abstract Hagfish intestinal antimicrobial peptides (HFIAPs) are a family of polycationic peptides exhibiting potent, broad-spectrum bactericidal activity. In an attempt to unravel the mechanism of action of HFIAPs, we have studied their interaction with model membranes. Synthetic HFIAPs selectively bound to liposomes mimicking bacterial membranes, and caused the release of vesicle-encapsulated fluorescent markers in a size-dependent manner. In planar lipid bilayer membranes, HFIAPs induced erratic current fluctuations and reduced membrane line tension according to a general theory for lipidic pores, suggesting that HFIAP pores contain lipid molecules. Consistent with this notion, lipid transbilayer redistribution accompanied HFIAP pore formation, and membrane monolayer curvature regulated HFIAP pore formation. Based on these studies, we propose that HFIAPs kill target cells, at least in part, by interacting with their plasma membrane to induce formation of lipid-containing pores. Such a membrane-permeabilizing function appears to be an evolutionarily conserved host-defense mechanism of antimicrobial peptides.

Key words: Antimicrobial peptides; Innate immunity; Cathelicidin; Hagfish; Lipidic pore; Membrane curvature

1. Introduction

Over the last 25 years, research has established that antimicrobial peptides are important components of the innate immune system in animals, playing a role in the first line of defense against invading microbes [1]. Although varying in length and primary structure, most antimicrobial peptides are polycationic at physiological pH, and adopt amphipathic secondary structures in which the cationic and hydrophobic residues segregate on opposite surfaces of α-helical or β-sheet motifs [2]. Such features enable these peptides to interact with the plasma membrane of target organisms and to breach this permeability barrier. Studies with synthetic peptide analogues and model lipid membranes have provided valuable insight into the mechanism(s) underlying membrane permeabilization by antimicrobial peptides. Several models have been proposed which can be classified in two general groups: formation of purely peptidic channels, and formation of lipid–peptide composite pores [1–4].

Hagfish intestinal antimicrobial peptides (HFIAPs) constitute an intriguing group of bioactive peptides. Isolated from a primitive fish lacking components of the vertebrate adaptive immune system, such as thymus tissue and immunoglobulin genes [5], HFIAPs are implicated as important components of the hagfish innate immune system [6]. Synthetic HFIAPs exhibit potent, broad-spectrum antibacterial activity but low activity against the prototypic fungus, *C. albicans* [6]. Their biosynthesis is localized in nests of hematopoietic cells within the intestinal submucosa, rather than in the epithelial lining of the hagfish gut, yet HFIAPs do not display significant hemolytic activity in vitro. Although native HFIAPs contain one or two residues of mono-brominated tryptophan, this unusual amino acid is not critical for conferring antimicrobial function (A.E. Shinnar et al., unpublished). Recent cDNA analysis of HFIAP clones shows that they are ancient ancestors of the cathelicidin gene family, for which members have been identified in various mammals, suggesting that their biological function has been evolutionarily conserved (T. Uzzell et al., unpublished).

In this work, the effect of HFIAPs on model lipid membrane systems has been investigated in order to elucidate their bactericidal mechanism of action. We show that HFIAPs bind to and induce permeabilization of vesicles mimicking membranes surface lipid compositions of bacteria but not of erythrocytes or *C. albicans*. We also present several lines of evidence supporting a model whereby, similar to magainin and analogous antimicrobial peptides, HFIAPs permeabilize membranes by forming pores containing bent lipid molecules.

2. Materials and methods

2.1. Materials

Dioleoylphosphatidylcholine (PC), dioleoylphosphatidylethanolamine (PE), dioleoylphosphatidylglycerol (PG), dioleoylglycerol (DG), oleoylphosphatidycholine (LPC), oleoylphosphatidylethanol-

*Corresponding author. Fax: +34 94 4648500.
E-mail address: gbzbaasg@lg.ehu.es (G. Basañez).

Abbreviations: ANTS, 8-aminonaphtalene-1,3,6-trisulfonate; CHOL, cholesterol; DG, dioleoylglycerol; DPX, *p*-xylene-bis-pyridinium bromide; FD-4, fluorescein isothiocyanate-labeled dextrans of ∼4 kDa; FD-70, fluorescein isothiocyanate-labeled dextrans of ∼70 kDa; HFIAP, hagfish intestinal antimicrobial peptide; LPC, oleoylphosphatidycholine; LPE, oleoylphosphatidylethanolamine; LUV, large unilamellar vesicles; OA, oleic acid; PC, dioleoylphosphatidylcholine; PE, dioleoylphosphatidylethanolamine; PG, dioleoylphosphatidylglycerol; Pyr-PC, 1-lauroyl-2-(1′ pyrenebutyroyl)-sn-glycero-3-phosphocholine; SM, sphingomyelin

0014-5793/02/$22.00 © 2002 Published by Elsevier Science B.V. on behalf of the Federation of European Biochemical Societies.
PII: S0014-5793(02)03651-7

amine (LPE), sphingomyelin (SM) and cholesterol (CHOL) were purchased from Avanti Polar Lipids (Alabaster, AL, USA). KCl, HEPES, EDTA, decane, Triton X-100, oleic acid (OA) and fluorescein isothiocyanate-labeled dextrans of ~4 kDa (FD-4) or ~70 kDa (FD-70) were from Sigma (St. Louis, MO, USA). 8-aminonaphtalene-1,3,6 trisulfonate (ANTS) and *p*-xylene-bis-pyridinium bromide (DPX) were from Molecular Probes (Eugene, OR, USA). 1-lauroyl-2-(1′pyrenebutyroyl)-sn-glycero-3-phosphocholine (Pyr-PC) was a kind gift of Dr. Andreas Herrman (Humboldt University, Berlin, Germany).

2.2. Synthetic peptides

Synthetic HFIAPs, prepared with native tryptophan, were provided by Genaera Corporation Sequences, corresponding to the C-terminally amidated peptides were: HFIAP-1 GFFKKAWRKVKHAGRRVLDTAKGVGRHYVNNWLNRYR; HFIAP-3 GWFKKAWRKVKNAGRRVLKGVGIHYGVGLI.

2.3. Liposome preparation and assays

Large unilamellar vesicles (LUV) were prepared by the freeze/thaw and extrusion method as described before [7]. Dry lipid films were resuspended in the following buffers: (i) membrane-binding assays: 100 mM KCl, 10 mM HEPES, pH 7.0, 0.2 mM EDTA (KHE), using D_2O instead of H_2O; (ii) release of vesicle contents: 12.5 mM ANTS, 45 mM DPX, 20 mM KCl, 10 mM HEPES, pH 7.0, 0.2 mM EDTA or KHE supplemented with 100 mg/ml FD; (iii) lipid flip-flop: KHE. For measuring HFIAP binding to LUV, peptides and vesicles were incubated together at 37°C for 30 min in D_2O buffer, and then the mixture was centrifuged at 200 000 × *g* at room temperature for 2 h. Under these conditions, vesicle-bound HFIAP remains with the upper fraction of the buffer, whereas free peptide sediments [8]. Peptide contents of LUV-associated or LUV-free fractions were estimated on the basis of the fluorescence intensities at $\lambda_{ex} = 280$ nm and $\lambda_{em} = 345$ nm, after addition of 0.5 mM $C_{12}E_{18}$ (dodecyl octaethyleneglycol mono ether). Fluorimetric assays were conducted in an 8100 SIM-Aminco instrument, using a thermostatted 1-cm path length cuvette with constant stirring at 37°C. Assays of vesicular release of fluorescent markers were performed as described in [7]. Experiments of pyPC transbilayer redistribution were done according to the method of Muller et al. [9].

2.4. Planar lipid bilayer membrane assays

Measurements were performed in decane-containing lipid bilayer membranes composed of egg phosphatidylethanolamine/egg phosphatidylglycerol (1:1), formed by the Mueller–Rudin technique across a 250-μm hole in a Lucite chamber (Warner, Hamden, CO, USA). KHE was used as the bathing solution. Membrane lifetime and line tension values were calculated as described in [10].

3. Results and discussion

3.1. Membrane-binding properties of HFIAP

HFIAPs are much more potent in inducing cell death of bacterial cells than of fungi or red blood cells [6]. The first step in the interaction of HFIAPs with any cell is the transfer of peptides from the extracellular environment to the cell surface. In order to mimic the primary lipid composition of the plasma membrane surfaces of bacteria [11], erythrocytes [12] and *C. albicans* [13], LUV composed of PE/PG (molar ratio 1:1), PC/CHOL/SM (1:1:1), and PC/CHOL (1:1) were used, respectively. HFIAPs associated with bacterial membrane mimetic LUV to a much greater extent than to erythrocyte or *C. albicans* membrane mimetic LUV (Fig. 1A). A distinguishing feature between the membranes of prokaryotic and eukaryotic organisms is that the former but not the latter contain negatively charged lipids in the outer leaflet of the cytoplasmic membrane [14]. To investigate whether electrostatic interactions are an important factor determining the membrane-binding capacity of HFIAPs, LUV containing various proportions of PC and PG were used. As shown in Table 1, the higher the proportion of PG in the liposomal membrane, the larger the amount of HFIAP-1 and HFIAP-3 bound to LUV. The extent of peptide binding is in line with their polycationic character, with HFIAP-1 and HFIAP-3 displaying a net charge of +12 and +9, respectively, at neutral pH. Thus, the selective cell-killing activity of HFIAPs against

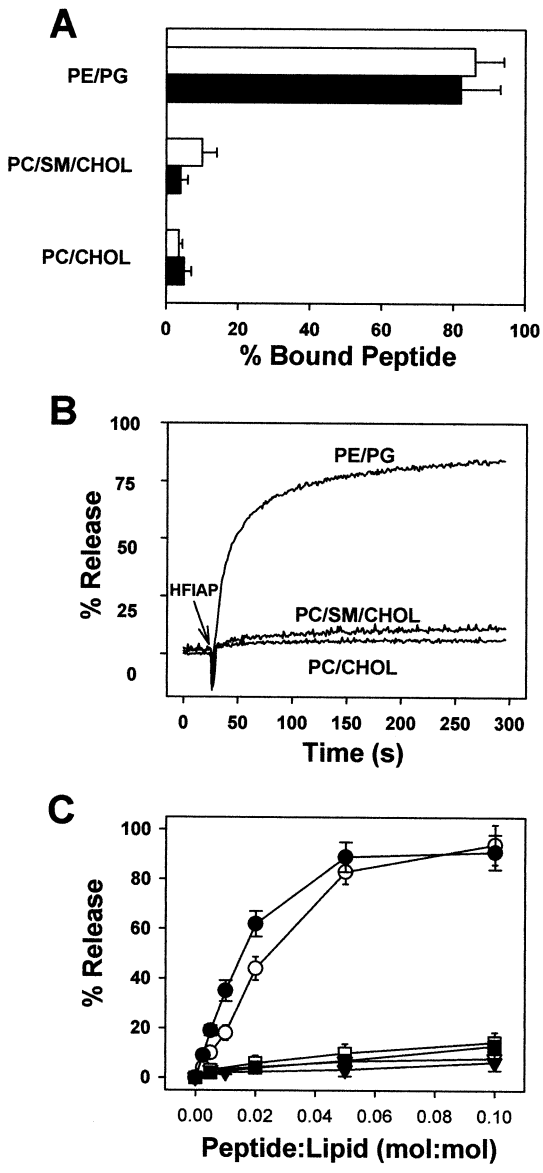

Fig. 1. Effect of HFIAPs in LUV emulating the outer leaflet lipid matrix of bacterial, erythrocyte, and *C. albicans* plasma membranes. A: Binding of HFIAP to LUV mimicking membranes of bacteria (PE/PG, molar ratio 1:1), erythrocytes (PC/SPM/CHOL, 1:1:1), and *C. albicans* (PC/CHOL, 1:1). Black bars, HFIAP-1; white bars, HFIAP-3. Lipid and peptide concentrations were 200 μM and 1 μM, respectively. Values represent mean values ± S.E.M. of duplicate experiments. B: Representative kinetics of HFIAP-1-induced ANTS release from PE/PG (1:1), PC/SM/CHOL (1:1:1), and PC/CHOL (1:1) LUV. Peptide and lipid concentrations were 1 μM and 25 μM, respectively. Similar results were obtained with HFIAP-3. C: Extents of ANTS release induced by HFIAP-1 (black symbols) and HFIAP-3 (white symbols) in LUV of PE/PG (1:1) (circles), PC/SM/CHOL (1:1:1) (squares) and PC/CHOL (triangles) at various peptide-to-lipid molar ratios. Concentration of lipid was 25 μM. Mean values ± S.E.M. values correspond to three to seven separate experiments.

Table 1
Comparison of the capacity of HFIAPs to bind to and permeabilize LUV of different lipid compositions

Lipid composition	HFIAP-1				HFIAP-3			
	% bound[a]	% release[b]			% bound	% release		
		ANTS	FD-4	FD-70		ANTS	FD-4	FD-70
PC	4 ± 1	5 ± 0	4 ± 0	0	9 ± 2	2 ± 1	0	N.D.
PC/PG (3/1)	29 ± 3	33 ± 5	26 ± 4	0	36 ± 6	28 ± 4	10 ± 1	0
PC/PG (1/1)	68 ± 8	74 ± 6	76 ± 8	8 ± 1	83 ± 7	69 ± 6	36 ± 2	0
PC/PG (1/3)	84 ± 7	85 ± 8	78 ± 6	17 ± 3	79 ± 7	91 ± 7	70 ± 9	0
PG	82 ± 9	93 ± 7	84 ± 9	25 ± 3	85 ± 9	89 ± 6	74 ± 7	6 ± 1
PE/PG (1/1)	80 ± 11	62 ± 5	50 ± 4	14 ± 2	86 ± 8	44 ± 4	13 ± 0	N.D.
PC/CHOL (1/1)	5 ± 2	3 ± 0	1 ± 0	1 ± 0	4 ± 1	3 ± 0	0	N.D.
PC/CHOL/SM (1/1/1)	4 ± 1	4 ± 0	6 ± 1	N.D.	11 ± 3	3 ± 1	2 ± 0	N.D.

Mean values ± S.E.M. shown for two to six independent experiments. N.D., not determined.
[a]Peptide and lipid concentrations were 1 μM and 200 μM, respectively.
[b]Peptide and lipid concentrations were 0.5 μM and 25 μM, respectively.

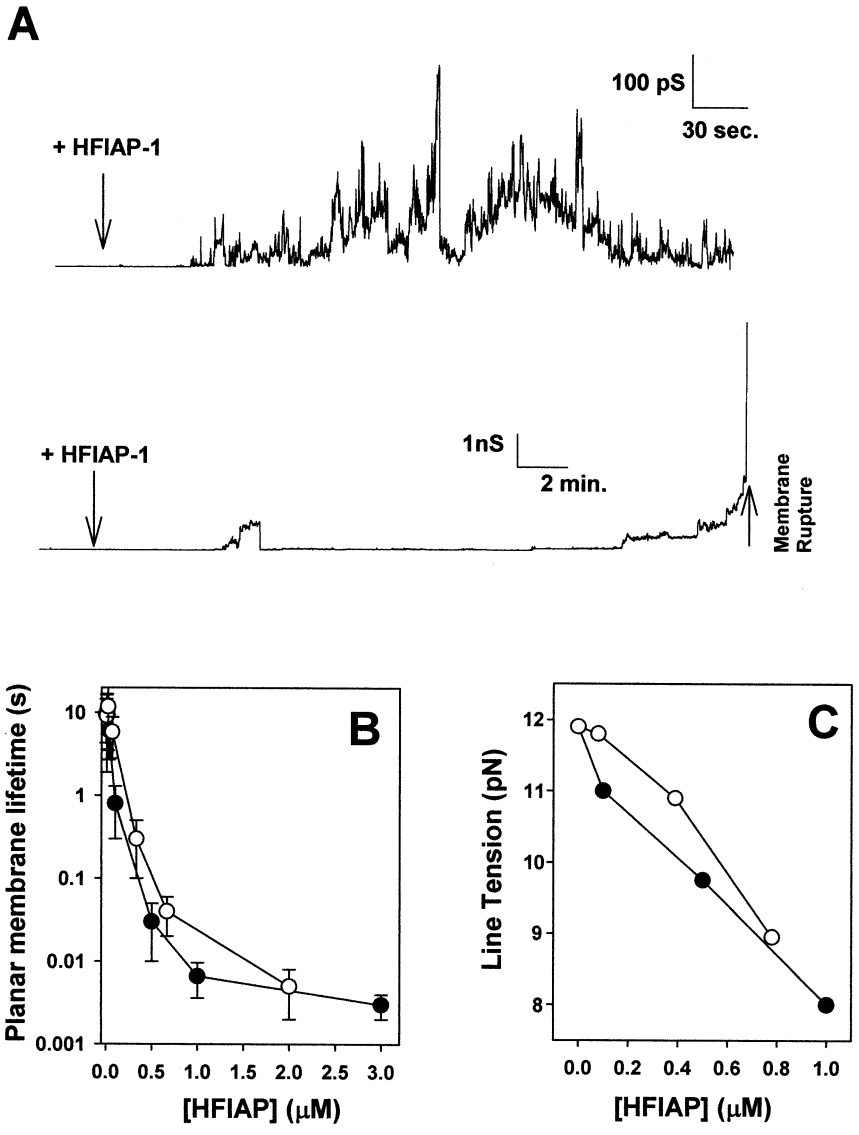

Fig. 2. Effect of HFIAPs in planar lipid bilayer membranes. A: Typical electrical activities observed after addition HFIAP-1 to a solution bathing a planar bilayer membrane. Note the different scales of the two current traces. The voltage in the top and bottom recordings was 50 mV and 130 mV, respectively. Peptide concentration was 300 nM in both cases. Lower peptide concentrations led to similar but delayed electrical responses. B: Dose-dependent decrease of membrane lifetime induced by HFIAP-1 (black circles) and HFIAP-3 (white circles). Voltage was 300 mV. All points are mean values ± S.E.M. ($n = 8$–12). C: Dose-dependent reduction of membrane line tension induced by HFIAP-1 (black circles) and HFIAP-3 (white circles).

bacteria is likely exerted at the level of electrostatic binding to the anionic membrane surface of these microorganisms.

3.2. LUV-permeabilizing properties of HFIAP

Once HFIAPs have reached the membrane surface, they may perturb the lipid bilayer permeability barrier, as other antimicrobial peptides apparently do [1–4]. To address this issue, LUV were loaded with the fluorescent marker ANTS and its quencher, DPX, and the release of ANTS from LUV was monitored as an increase in the fluorescence of the dye due to its dilution in the external medium. HFIAPs caused fast and extensive release of ANTS from PE/PG (1:1) LUV (Fig. 1B). In such LUV, the onset of ANTS release took place at a peptide-to-lipid molar ratios of approximately 1/200 (Fig. 1C). Maximum dye release occurred, however, at about 1/20 peptide/lipid molar ratio, probably when the peptide covers the whole liposome surface in a carpet-like manner [3]. In contrast, HFIAPs were much less effective in causing ANTS release from PC/SM/CHOL (1:1:1) LUV or PC/CHOL (1:1) LUV. Therefore, both the binding of HFIAPs to LUV mimicking biological membranes and also the capacity of HFIAPs to release vesicle-encapsulated ANTS from those LUV are in line with their biological activity.

Next, we wished to explore whether the net charge of the membrane is important for HFIAP-induced permeabilization, as well as whether the membrane lesion caused by HFIAPs is sizable. To this aim, LUV containing varying amounts of PC and PG were loaded with ANTS/DPX, FD-4, or FD-70. As in the membrane-binding experiments, the higher the amount of PG, the larger the extent of HFIAP-induced LUV permeabilization (Table 1). In PG-containing LUV, the HFIAP-1-induced permeability pathway allowed similar extents of ANTS and FD-4 release but a more limited release of FD-70. On the other hand, the HFIAP-3-induced permeability pathway allowed FD-4 release to a somewhat lesser extent than ANTS, and did not allow FD-70 release. Because the permeability pathways induced by HFIAPs in LUV discriminate permeants according to size, these results imply that under these conditions HFIAPs induce vesicle contents release through a channel/pore mechanism, without causing the total destruction of the liposomal membrane. In agreement with this, HFIAPs did not seem to cause major changes in vesicle structure or morphology, as deduced from dynamic and static light scattering measurements of LUV before and after peptide treatment (data not shown).

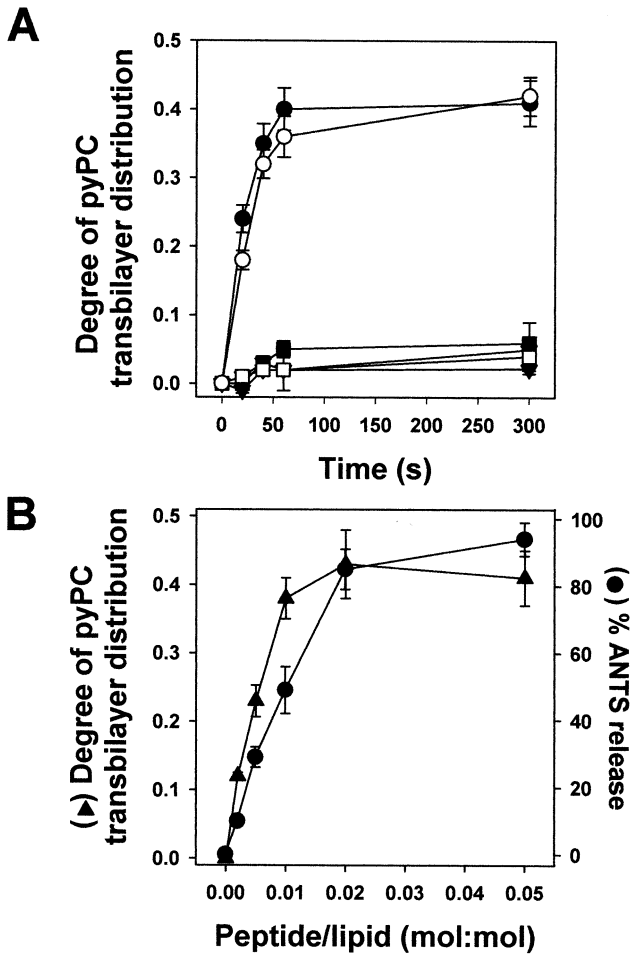

Fig. 3. Influence of HFIAPs on lipid transbilayer redistribution. A: Time course of the transbilayer distribution of pyPC in LUV composed of PE/PG (1:1) (circles), PC/SM/CHOL (1:1:1) (squares), or PC/CHOL (1:1) (triangles) in the presence of HFIAP-1 (black symbols) or HFIAP-3 (white symbols). LUV were labeled in the outer leaflet by external addition of pyPC (5 mol% of total lipid) to the liposome suspension, and the degree of transbilayer redistribution of pyPC at any given time was estimated from the ratio between excimer and monomer fluorescence intensity signals. Concentrations of peptide and lipid were 0.5 μM and 25 μM, respectively. At comparable timescales there was no measurable transbilayer movement of pyPC in the absence of peptides. B: Comparison of the HFIAP-1-induced pyPC transbilayer redistribution (triangles) and ANTS release (circles) at different peptide-to-lipid molar ratios. LUV composition was PC/PG (1:1) and lipid concentration was 25 μM.

3.3. Planar lipid bilayer membrane electrophysiology of HFIAPs

To gain more insight into the mechanism of membrane permeabilization induced by HFIAPs, electrophysiology of planar lipid bilayer membranes was used. Addition of HFIAPs to a solution bathing a planar bilayer led to increased membrane conductance (Fig. 2A). Typically, noise-like fluctuations were observed, which were characterized by continuously variable conductance levels (Fig. 2A, top trace). In addition, a tendency for instability was noted in HFIAP-treated planar membranes, especially at relatively high transmembrane voltages (Fig. 2A, bottom trace).

The results obtained with HFIAPs in planar membranes are unexpected for ion channels, which typically induce more reproducible changes in membrane conductance and do not decrease membrane stability. An alternative explanation is that membrane lipids are involved in HFIAP pore formation. Indeed, the behavior observed for HFIAP-treated planar membranes is reminiscent of membranes modified by certain peptides and proteins thought to form lipid-containing pores rather than purely proteinaceous channels [7,10,15–17]. To further explore this possibility, a general model for lipidic pores and lipid bilayer rupture was considered, where pore enlargement is determined by a balance between membrane surface tension, decreasing pore energy, and favoring membrane rupture, and membrane line tension, increasing pore energy, and opposing membrane rupture [18]. By fitting the voltage dependence of membrane lifetime (i.e. the duration of the membrane until collapse) to a theoretical expression for lipidic pore enlargement, line tension values can be obtained. Both HFIAP-1 and HFIAP-3 decreased membrane lifetime at

submicromolar concentrations (Fig. 2B). Moreover, membrane line tension progressively diminished as the amount of HFIAPs increased, reducing its original value by ~35% and ~25% at HFIAP-1 and HFIAP-3 concentrations of 1.0 μM and 0.78 μM, respectively (Fig. 2C). It is worth emphasizing here that even small changes in line tension should significantly affect the probability of lipidic pore formation [18]. Thus, these results support the view that HFIAPs form pores in the membrane together with lipid molecules.

3.4. HFIAP cause lipid transbilayer redistribution

One implication of the lipidic pore concept is that its formation would allow the movement of lipid molecules from one monolayer of the bilayer to the other. To address this issue, the fluorescent phosphatidylcholine analog pyPC was employed. Membrane-incorporated pyPC displays two distinct peaks in the fluorescence spectrum, one arising from excited monomeric pyPC molecules and the other arising from excited dimeric (excimer) pyPC molecules [9]. The transbilayer movement of pyPC can be estimated from the ratio of the excimer to monomer fluorescence intensity signals. Addition of HFIAPs to PE/PG (1:1) LUV containing pyPC localized exclusively in the external monolayer led to a rapid transfer of the fluorescent analog to the internal monolayer (Fig. 3A). On the other hand, the transbilayer movement of pyPC was not increased in PC/SM/CHOL (1:1:1) or PC/CHOL (1:1) vesicles, paralleling the results obtained in ANTS release experiments. Moreover, in PG-containing LUV, HFIAPs elicited the transbilayer redistribution of pyPC with similar kinetics and at comparable peptide-to-lipid ratios to those obtained in analogous ANTS release experiments (Fig. 3B, and data not shown). Thus, these results strongly suggest that HFIAP-caused LUV permeabilization and lipid transbilayer relocation are mechanistically related phenomena.

3.5. Non-bilayer lipids affect HFIAP-induced membrane permeabilization

If, as suggested by the results discussed above, HFIAPs form lipid-containing pores, their membrane-permeabilizing activities should be sensitive to the lipid composition of the membrane and, thus, to the physicochemical properties of the lipid bilayer. In particular, the membrane monolayer must bend during lipidic pore formation [18]. Lipid monolayers can be bent in two directions, termed negative and positive curvature by convention [19], and membrane permeability can be breached by increasing both types of monolayer curvature [20]. To assess whether membrane monolayer curvature is important for HFIAP pore formation, LUV containing curvature-inducing lipids (non-bilayer lipids) were employed. Non-bilayer lipids having positive intrinsic curvature such as LPC and LPE generally promoted HFIAP-induced vesicular ANTS release, whereas non-bilayer lipids having negative intrinsic curvature such as DG and OA had the opposite effect (Fig. 4A). The effect of LPC, LPE, DG, and OA on HFIAP-induced LUV permeabilization correlated well with their relative tendency for curvature [21–23]. It is noteworthy that a number of antimicrobial peptides, exemplified by magainin, have been shown to form pores displaying a dependence on curvature similar to that observed with HFIAPs [2,4].

Since the intrinsic curvature of LPC is opposite to that of DG, further experiments focused on whether LPC and DG counterbalance each other's effects on LUV permeabilization.

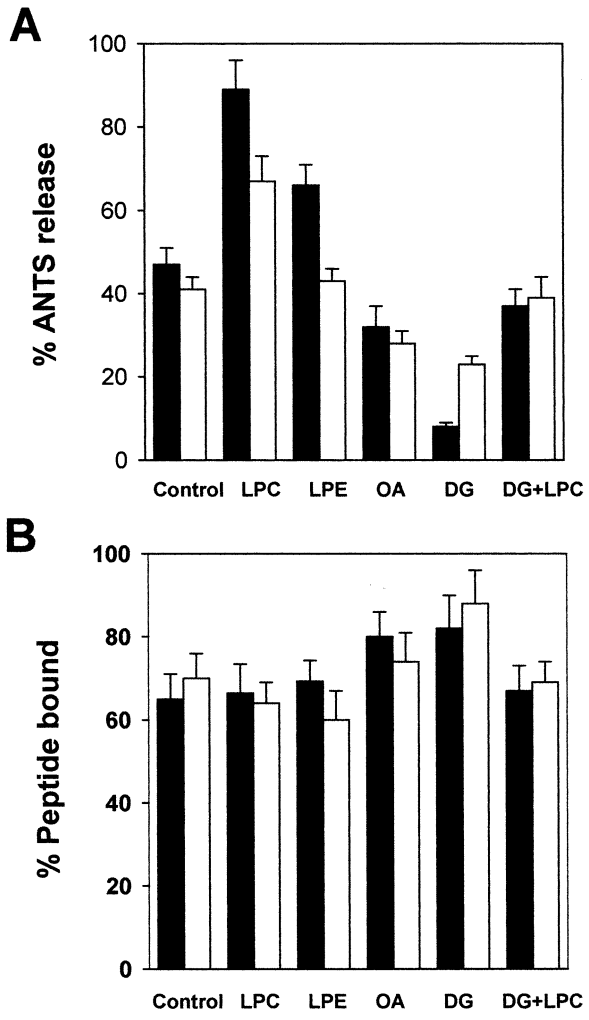

Fig. 4. Effect of non-bilayer lipids on HFIAP-induced LUV permeabilization. A: Extents of ANTS release elicited by HFIAP-1 (black bars) and HFIAP-3 (white bars) in LUV of PC/PG (5/5) (control), PC/PG/LPC (4/5/1) (LPC), PC/PG/LPE (4/5/1) (LPE), PC/PG/OA (4/5/1) (OA), PC/PG/DG (4/5/1) (DG), and PC/PG/DG/LPC (2/5/1/2) (DG+LPC). Peptide and lipid concentrations were 0.25 μM and 25 μM, respectively. Mean values ± S.E.M. of four independent experiments are shown. B: Effect of non-bilayer lipids on the binding of HFIAPs to LUV. Mean values ± S.E.M. of three separate experiments are shown. The rest of the conditions are as in A.

In agreement with this prediction, HFIAPs induced the release of ANTS to similar extents in LUV containing both DG and LPC and in control LUV (Fig. 4A). Since the effects of non-bilayer lipids on HFIAP-induced LUV permeabilization could be due to changes in the peptide affinity for the membrane, binding studies were also carried out. As shown in Fig. 4B, however, differences in the capacity of HFIAPs to bind LUV were not correlated with differences in HFIAP-induced vesicular ANTS release.

In summary, our investigations reveal that HFIAPs (1) form relatively large permeability pathways in the membrane of LUV which allow a size-dependent efflux of vesicle-entrapped markers, (2) induce continuously variable conductance changes in planar membranes, with a reduction of planar membrane lifetime and line tension as expected for lipidic pores, and (3) cause lipid transbilayer redistribution concomitant with vesicular contents release through a mechanism

sensitive to changes in membrane monolayer curvature. Thus, it seems highly plausible that HFIAPs permeabilize membranes by forming pores lined, at least in part, with lipid molecules. Our findings of such a membrane-permeabilizing activity in antimicrobial peptides of a primitive fish adds to the growing body of evidence suggesting that formation of lipid-containing pores is a widespread, evolutionarily conserved mechanism for antimicrobial peptide action [1–4,24].

Acknowledgements: We are grateful to Dr. W. Lee Maloy and members of Peptide Chemistry at Genaera Corporation for the gift of synthetic peptides used in these studies. This study was supported in part by the Ministerio de Ciencia y Tecnología and by the Universidad del País Vasco (UPV/EHU) (Spain).

References

[1] Zasloff, M. (2002) Nature 415, 389–395.
[2] Epand, R.M. and Vogel, H.J. (1999) Biochim. Biophys. Acta 1462, 11–28.
[3] Shai, Y. and Oren, Z. (2001) Peptides 40, 12591–12603.
[4] Matsuzaki, K. (1998) Biochim. Biophys. Acta 1376, 391–400.
[5] Raison, R.L. and dos Remedios, N.J. (1998) in: The Biology of Hagfishes (Jørgensen, J.M, Lomholt, J.P., Weber, R.E., and Malte, H., Eds.), pp. 334–344, Chapman and Hall, London.
[6] Shinnar, A.E., Uzzell, T., Rao, M.N., Spooner, E., Lane, W.S. and Zasloff, M.A. (1996) in: Peptides: Chemistry and Biology, Proc. 14th Am. Peptide Symp. (Kauyama, P. and Hodges, R., Eds.), pp. 189–191, Mayflower Scientific, Leiden.
[7] Basañez, G., Zhang, J., Chau, B.N., Maksaev, G.I., Frolov, V.A., Brandt, T.A., Burch, J., Hardwick, J.M. and Zimmerberg, J. (2001) J. Biol. Chem. 276, 31083–31091.
[8] Pereira, F.B., Goni, F.M. and Nieva, J.L. (1995) FEBS Lett. 362, 243–246.
[9] Muller, P., Schiller, S., Wieprecht, T., Dathe, M. and Herrmann, A. (2000) Chem. Phys. Lipids 106, 89–99.
[10] Basañez, G., Nechushtan, A., Drozhinin, O., Chanturiya, A., Choe, E., Tutt, S., Wood, K.A., Hsu, Y., Zimmerberg, J. and Youle, R.J. (1999) Proc. Natl. Acad. Sci. USA 96, 5492–5497.
[11] O' Leary, W.M. and Wilkinson, S.G. (1988) in: Microbial Lipids (Ratledge, C. and Wilkinson, S.G., Eds.), Vol. 1, pp. 117–201, Academic Press, London.
[12] Opden Camp, J.A.F. (1979) Annu. Rev. Biochem. 48, 47–71.
[13] Dogra, S., Krishnamurthy, S., Gupta, V., Dixit, B.L., Gupta, C.M., Sanglard, D. and Prasad, R. (1999) Yeast 15, 111–121.
[14] Yorek, M.A. (1993) in: Phospholipids Handbook (Cevc, G., Ed.), pp. 745–775, Marcel Dekker, New York.
[15] Basañez, G. and Zimmerberg, J. (2001) J. Exp. Med. 193, F11–F14.
[16] Chernomordik, L., Chanturiya, A.N., Suss-Toby, E., Nora, E. and Zimmerberg, J. (1994) J. Virol. 68, 7115–7123.
[17] Kudla, G., Montessuit, S., Eskes, R., Berrier, C., Martinou, J.C., Ghazi, A. and Antonsson, B. (2000) J. Biol. Chem. 275, 22713–22718.
[18] Chernomordik, L.V., Kozlov, M.M., Melikyan, G.B., Abidor, I.G., Markin, V.S. and Chizmadzhev, Y.A. (1985) Biochim. Biophys. Acta 812, 643–655.
[19] Basañez, G. (2002) Cell. Mol. Life Sci. 59, 1478–1490.
[20] Epand, R.M. (1998) Biochim. Biophys. Acta 1376, 353–368.
[21] Fuller, N.L. and Rand, P.R. (2001) Biophys. J. 81, 243–254.
[22] Szule, J.A., Fuller, N.L. and Rand, P.R. (2002) Biophys. J. 83, 977–984.
[23] Epand, R.M., Epand, R.F., Ahmed, N. and Chen, R. (1991) Chem. Phys. Lipids 57, 75–80.
[24] Yang, L., Harroun, T.A., Weiss, T.M., Ding, L. and Huang, H.W. (2001) Biophys. J. 81, 1475–1485.